



## MECHANICS AND MATERIALS SCIENCE

## МЕХАНІКА ТА МАТЕРІАЛОЗНАВСТВО

UDC 539.3

### EXPERIMENTAL STUDY OF PSEUDOELASTIC NITI ALLOY UNDER CYCLIC LOADING

Volodymyr Iasnii<sup>1</sup>; Petro Yasnii<sup>1</sup>; Yuri Lapusta<sup>2</sup>; Tetiana Shnitsar<sup>1</sup>

<sup>1</sup>Ternopil Ivan Puluj National Technical University, Ternopil, Ukraine

<sup>2</sup>French institute of advanced mechanics, Clermont-Ferrand, France

**Summary.** The phase transformation temperatures of pseudoelastic NiTi alloy were defined by differential scanning calorimetry. The effect of the stress range on the functional properties of the NiTi alloy under uniaxial tension in ice water at a temperature of 0°C was studied. The cylindrical specimens with 4 mm in diameter and a gage length of 12.5 mm were tested under static and cyclic loading with frequency of 0.5 Hz. All cyclic tests were performed under the crosshead displacement controlled condition on the STM100 machine. At the temperature above  $A_f$  the effect of the cyclic loading on the maximum stress in general could be characterized by several stages: strengthening, softening, stabilization and rapid decrease of the maximum stress, which is caused by the initiation and macrocrack growth. With the increase of the maximal stress in the first cycle from 509 MPa to 605 MPa, the strain range also increases.

**Key words:** NiTi alloy, pseudoelasticity, differential scanning calorimetry, functional properties, maximal; stresses, strain range.

[https://doi.org/10.33108/visnyk\\_tntu2018.04.007](https://doi.org/10.33108/visnyk_tntu2018.04.007)

Received 09.01.2019

**Statement of the problem.** Shape memory alloys (SMA) belong to functional materials characterized by the shape memory effect and pseudoelasticity. Their application depends on the temperature of phase transformations, mechanical and functional properties, the type of load (static, cyclic and thermomechanical).

Due to the high ability to dissipation energy the SMA with the effect of pseudoelasticity are increasingly used in parts of machines, implants [1], damping devices [2 – 4] or other structuralelements [5]. Since they are subjected to intense cyclic loadings during operation, it is important to ensure their reliability and durability for low-cycle fatigue.

Therefore, in order to construct the structural elements and devices made of SMA it is necessary to study the regularities of changing stress and strain based parameters, which characterize functional properties..

**Analysis of available investigation results.** It is known that with the increase of load cycles number, the SMA functional properties (hyperelasticity effect) which can be characterized by the strain range, residual strain [6] get worse. The effect of maximum stress, mean stress and stress amplitude on SMA cyclic behavior is investigated. It is determined that the maximum strain depends in general on the stress level and load type.

Particularly, residual and transformation hardening increase with the growth of loading cycles number and strain rates from  $3,3 \cdot 10^{-4} \text{ s}^{-1}$  до  $3,3 \cdot 10^{-2} \text{ s}^{-1}$  in super-elastic NiTi SMA micro-tube (50.32% Ni) specimens in 2.5 mm in diameter during strain-controlled testing [7].

The residual strain growth was also observed for low-cycle fatigue of the wire made of NiTi alloy under uniaxial tension [8].

The residual deformation is usually considered to be related with some oriented martensite, which is not transformed back into austenite during the reverse phase [9]. Repeated changes in the direct and reciprocal phases create some defects in the material [10] resulting in localized internal stresses [11] allowing SMA to detect double-sided memory effect.

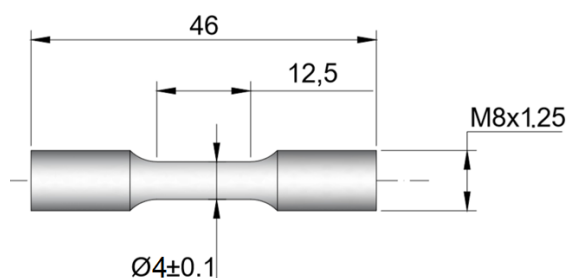
**The objective of the paper.** The influence of the stress range on functional properties of Ni<sub>55,8</sub>Ti<sub>44,2</sub> alloy at temperature higher than the temperature of austenitic transformation completion is investigated experimentally.

**Research techniques.** The effect of cyclic loading on Ni<sub>55,8</sub>Ti<sub>44,2</sub> alloy functional properties in the form of 8 mm diameter rod supplied by Wuxi Xin Xin glai Steel Trade Co., LTD (China) was investigated. The chemical composition of the alloy, stated in the certificate: 55,78% Ni; 0,005% Co; 0,005% Cu; 0,005% Cr; 0,012% Fe; 0,005% Nb; 0,032% C; 0,001% H; 0,04% O; 0,001% N; 44,12% Ti.

Characteristics of thermal transitions during SMA phase transformations were investigated using Differential Scanning Calorimetry (DSC) [12] by means of DSC Q1000. The cylindrical specimen 1 mm in diameter with one flat side and 17,2 mg weight cut from Ø 8 mm rod were placed on a crucible plate made of Al<sub>2</sub>O<sub>3</sub>. Gas flow velocity was 30 ml/min. The specimen was heated and cooled from -150 to +120°C in nitrogen atmosphere N<sub>2</sub> and helium He<sub>2</sub> at 10°C/min rate. To increase the reliability of the obtained results, each of the heating and cooling cycles was repeated three times.

Mechanical properties and cyclic loading influence on the functional properties of NiTi alloy were investigated at 0°C temperature under the uniaxial tension of cylindrical specimens 4 mm diameter and 12.5 mm operating area length cut from Ø 8 mm rod (Fig.1a). The specimens were tested on the servohydraulic machine STM-100 [13] with automated control and data acquisition system under maximum uniform stem shifting with 0.5 Hz load frequency and sinusoidal cycle shape. Asymmetry coefficient of the load cycle  $r = s_{\min} / s_{\max} = 0$  (here  $s_{\min}$ ,  $s_{\max}$  is the least and the largest value of the stem shifting). During the tests for the first and the following load cycles at  $s_{\min} = 0$ , the strains in the specimens were not observed.

During the test, the current values of force, stem shifting and the longitudinal deformation of the specimen operating area with 12 mm measuring base were recorded. Longitudinal deformation was measured by Bi-06-308 extensometer produced by BISS, maximum error did not exceed 0.1%. The stem shifting was determined by inductive Bi-02-313 sensor with an error not more than 0.1%. The tests were carried out in the chamber filled with ice and ice water (Fig.1b). This provided the steady temperature of 0°C measured by chromel-alumel thermocouple mounted on the specimen with an error not more than 0,5°C.



a



b

**Figure 1.** Specimen for fatigue tests – a; chamber with ice water for cooling the specimen installed with extensometer on the STM-100 machine – b

**Results and their discussion.** DSC analysis in coordinates heat-temperature (F–T): the curves demonstrate the martensitic-austenitic (Fig. 2a) and austenitic-martensitic (Fig. 2b) phase transformations occurring in SMA during the heating and cooling cycles relatively. Comparison of the phase transition temperatures confirms the reversible nature of the change in the crystallographic structure of the investigated material. While heating the specimen, the phase transition takes place in temperature range between  $-60,5^{\circ}\text{C}$  and  $-38,7^{\circ}\text{C}$  (extrapolation of the average value), and transition temperature is  $-45,7^{\circ}\text{C}$ . The reverse phase transition during cooling is between  $-95,9^{\circ}\text{C}$  and  $-69,4^{\circ}\text{C}$  and the heat flow reaches its maximum at  $-81,4^{\circ}\text{C}$ .

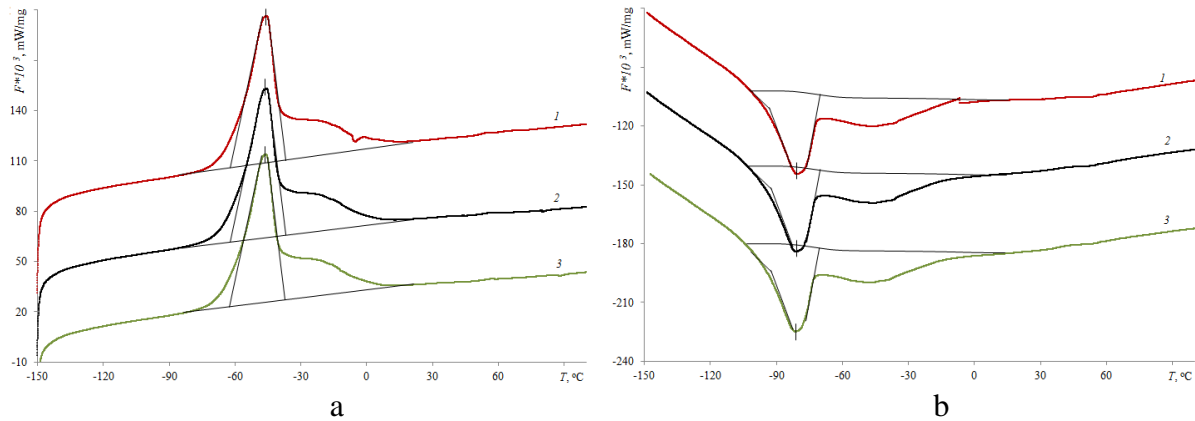


**Figure 2.** DSC analysis during first (1), second (2) and third (3) heating (a) and cooling (b) mode

The enthalpy change caused by phase transformations was  $12,43 \text{ J/g}$  during heating and  $11,07 \text{ J/g}$  for cooling (Fig. 3).

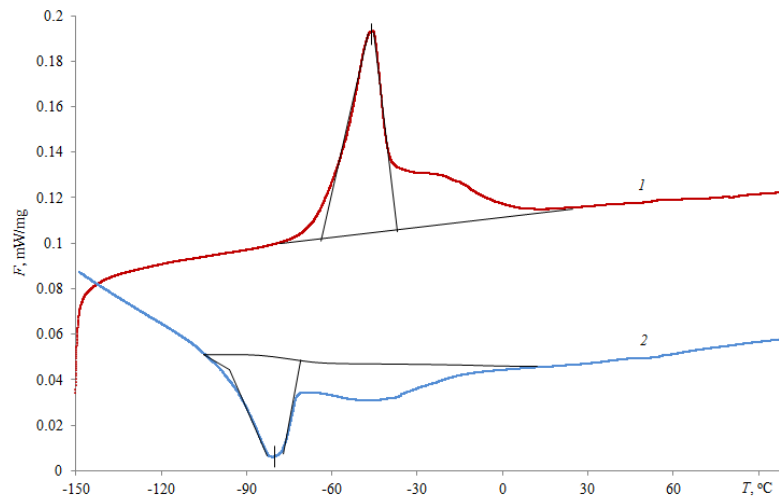


**Figure 3.** Enthalpy change during phase transformation of SMA in heating (1) and cooling (2) mode

Summarized results of the phase transformation temperatures of the investigated SMA are given in Table 1. Here  $M_s$ ,  $M_f$ ,  $A_s$ ,  $A_f$  are the start and end temperatures of the martensitic and austenitic phase, respectively. It should be noted that the temperature of the phase transformations in the wire material has a slight dispersion between separate heating (cooling) cycles. Thus, the maximum deviation from the average temperature value of  $A_f$  austenitic transformation completion is  $0,3^{\circ}\text{C}$  and for  $M_f$  is  $0,7^{\circ}\text{C}$ .

**Table 1**

Temperature of phase transformations in NiTi alloy

Heating / cooling	$M_s$	$M_f$	$A_s$	$A_f$
	°C			
1-e	-68,7	-95,5	-60,3	-38,5
2-e	-69,6	-95,9	-60,5	-38,5
3-ε	-70,0	-96,2	-60,6	-39,0
Averaged value	-69,4	-95,9	-60,5	-38,7

Characteristics of the mechanical properties of the alloy were determined according to standard [14] at 0°C temperature which was higher than the temperature of the martensitic-austenitic transformation completion  $A_f = -38,7^\circ\text{C}$  (Table 1).

The stretch diagram (Fig. 4) consists of three sections: I – elastic behaviour (austenitic phase); II – pseudoelastic (austenitic-martensitic phase), where the properties of hyperelasticity are observed; III – elasto-plastic deformation (martensitic phase), which results the specimen fracture.

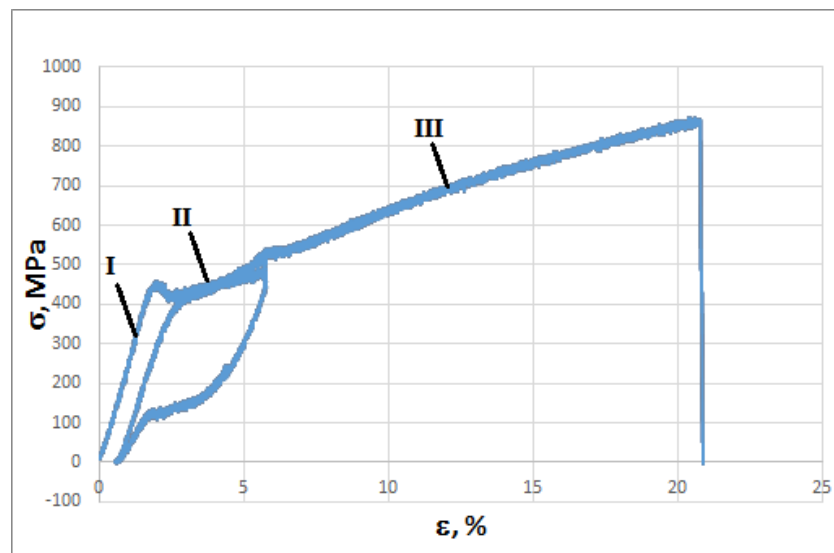


**Figure 4.** Stress-strain diagrams of SMA at 0 °C: I – austenitic phase; II – austenite-martensitic; III – martensitic

Characteristics of the alloy mechanical properties are given in Table. 2

**Table 2**

Mechanical properties of NiTi alloy at 0°C

Yield Strength, $\sigma_{0,2}$	Ultimate Tensile Strength, $\sigma_{UTS}$	Young's Modulus, GPa	
MPa		I section	II section
447	869	25,3	16,9

Dependencies of the maximum stress  $\sigma_{\max}$  and strain range of SMA on the number of load cycles for different starting values  $\sigma_{\max} = \sigma_1$  are shown in Fig. 5 a,b. For all values of the initial maximum stress, during the first load cycles, the growth of in  $\sigma_{\max}$  value (material strengthening) is observed, then the weakening and stabilization, followed by the decrease section in the maximum stress caused by the macrocrack initiation and its growth. An exception is only the specimen with the initial maximum stress  $\sigma_1 = 748$  MPa, which continuously decreased during operation time.

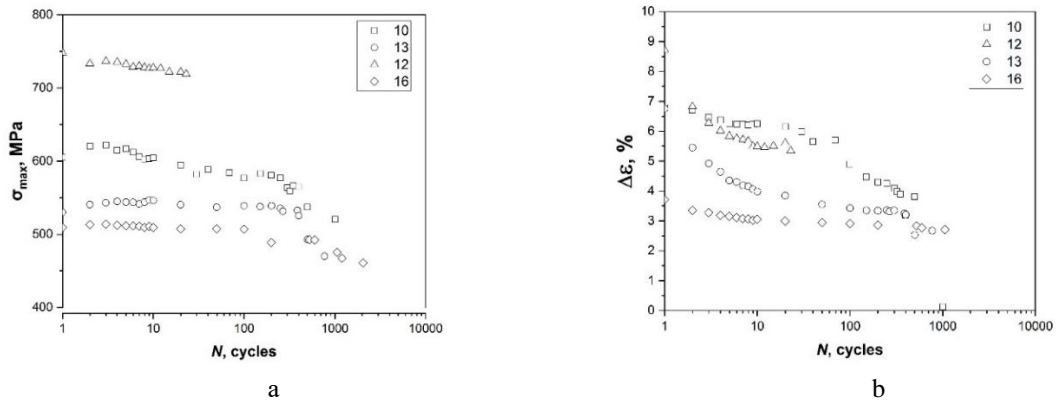


**Figure 5.** Dependencies of the maximum stress – a and strain range – b on the number of loading cycles of SMA for  $\sigma_1 = 509$  MPa (16) MPa, 530 MPa (13), 605 MPa (10), 748 MPa (12). Number of specimen are indicated in brackets

Functional properties of the shape memory alloy (hyperelasticity) can be characterized particularly by the magnitude of strain range per cycle.

For all values of the initial maximum stress, during the first ten load cycles there is a rapid decrease in the strain range followed by the stabilization area of the strain range or its less intensive decrease followed by a recession area resulting in the specimen fracture (Fig. 5b). With the increase of the maximum stress in the first load cycle from 509 MPa to 605 MPa, the strain range value increases (Fig. 5b).

In general, the strain range depends on the initial maximum stress, with the increase of which the strain range increases.

### Conclusions.

1. The temperature of forward and reverse phase transitions of pseudoelastic NiTi alloy is determined by differential scanning calorimetry technique.
2. The influence of stress range on the strain regularities and functional properties of pseudoelastic NiTi alloy in ice water at 0°C is studied and appropriate methodology is developed.
3. At the temperature higher than the temperature of martensitic-austenitic transformation finish under controlled crosshead displacement, the influence of the cyclic loading on the maximum stress can be characterized in general by areas of strengthening, weakening, stabilization and rapid decrease of the maximum stress caused by fatigue macrocrack initiation and extension.
4. The rapid decrease of the strain range observed during first ten loading cycles, without regard to the initial value of the maximum stress, followed by the stabilization area, which changes into the area of continuous strain range reducing, ending with fracture of specimen.

### Reference

1. Auricchio F., Boatti E., Conti M. SMA Biomedical Applications // Shape Mem. Alloy Eng. Butterworth-Heinemann, 2015. P. 307 – 341. <https://doi.org/10.1016/B978-0-08-099920-3.00011-5>
2. Yasniy P. et al. Calculation of constructive parameters of SMA damper // Sci. J. TNTU. 2017. Vol. 88, № 4. P. 7 – 15. [https://doi.org/10.33108/visnyk\\_tntu2017.04.007](https://doi.org/10.33108/visnyk_tntu2017.04.007)
3. Torra V. et al. The SMA: An Effective Damper in Civil Engineering that Smooths Oscillations // Mater. Sci. Forum. 2012. Vol. 706 – 709, № July 2015. P. 2020 – 2025. <https://doi.org/10.4028/www.scientific.net/MSF.706-709.2020>

4. Isalgue A. et al. SMA for Dampers in Civil Engineering // Mater. Trans. 2006. Vol. 47, № 3. P. 682 – 690. <https://doi.org/10.2320/matertrans.47.682>
5. Menna C., Auricchio F., Asprone D. Applications of shape memory alloys in structural engineering // Shape Memory Alloy Engineering. 2015. 369 – 403 p. <https://doi.org/10.1016/B978-0-08-099920-3.00013-9>
6. Kang G. et al. Whole-life transformation ratchetting and fatigue of super-elastic NiTi Alloy under uniaxial stress-controlled cyclic loading // Mater. Sci. Eng. A. Elsevier, 2012. Vol. 535. P. 228 – 234. <https://doi.org/10.1016/j.msea.2011.12.071>
7. Kan Q. et al. Experimental observations on rate-dependent cyclic deformation of super-elastic NiTi shape memory alloy // Mech. Mater. Elsevier, 2016. Vol. 97. P. 48 – 58. <https://doi.org/10.1016/j.mechmat.2016.02.011>
8. Moumni Z., Zaki W., Maitournam H. Cyclic Behavior and Energy Approach to the Fatigue of Shape Memory Alloys // J. Mech. Mater. Struct. 2009. Vol. 4, № 2. P. 395 – 411. <https://doi.org/10.2140/jomms.2009.4.395>
9. Auricchio F., Marfia S., Sacco E. Modelling of SMA materials: training and two way memory effect. // Comput. Struct. 2003. Vol. 81. P. 2301 – 2317. [https://doi.org/10.1016/S0045-7949\(03\)00319-5](https://doi.org/10.1016/S0045-7949(03)00319-5)
10. Abeyaratne R., Kim S.-J. Cyclic effects in shape-memory alloys: a one-dimensional continuum model // Int. J. Solids Struct. Pergamon, 1997. Vol. 34, № 25. P. 3273 – 3289. [https://doi.org/10.1016/S0020-7683\(96\)00213-2](https://doi.org/10.1016/S0020-7683(96)00213-2)
11. Tanaka K. et al. Phenomenological analysis on subloops and cyclic behavior in shape memory alloys under mechanical and/or thermal loads // Mech. Mater. Elsevier, 1995. Vol. 19, № 4. P. 281 – 292. [https://doi.org/10.1016/0167-6636\(94\)00038-1](https://doi.org/10.1016/0167-6636(94)00038-1)
12. Iasnii V., Junga R. Phase Transformations and Mechanical Properties of the Nitinol Alloy with Shape Memory // Mater. Sci. 2018. Vol. 54, № 3. P. 406 – 411. <https://doi.org/10.1007/s11003-018-0199-7>
13. YASNIY P.V. et al. Microcrack initiation and growth in heat-resistant 15Kh2MFA steel under cyclic deformation // Fatigue Fract. Eng. Mater. Struct. Blackwell Science Ltd, 2005. Vol. 28, № 4. P. 391 – 397. <https://doi.org/10.1111/j.1460-2695.2005.00870.x>
14. ASTM F2516-14. Standard Test Method for Tension Testing of Nickel-Titanium Superelastic Materials. Book of Standards Volume: 13.02. 2014.

## УДК 539.3

### ДОСЛІДЖЕННЯ НАДПРУЖНОЇ ПОВЕДІНКИ NITИ СПЛАВУ ЗА ЦИКЛІЧНОГО НАВАНТАЖЕННЯ

Володимир Ясній<sup>1</sup>; Петро Ясній<sup>1</sup>; Юрій Лапуста<sup>2</sup>; Тетяна Шніцар<sup>1</sup>

<sup>1</sup>Тернопільський національний технічний університет імені Івана Пулюя, Тернопіль, Україна

<sup>2</sup>Інститут сучасної механіки, Клермон-Ферран, Франція

**Резюме.** Методом диференціальної сканувальної калориметрії досліджено температуру прямих і зворотних фазових переходів нікельтитанового сплаву Ni<sub>55,8</sub>Ti<sub>44,2</sub>. Зіставлення температур фазових переходів підтверджує зворотний характер зміни кристалографічної структури досліджуваного матеріалу. Під час нагрівання зразка фазовий перехід відбувається в діапазоні температур між -60,5 °C та -38,7 °C, а температура переходу становить -45,7 °C. Таким чином, температури початку і завершення аустенітної фази склали відповідно A<sub>s</sub> = -60,5 °C і A<sub>f</sub> = -38,7 °C. Розроблено методику й досліджено вплив розмаху напруження на закономірності деформування одноосним розтягом і функціональні властивості нікельтитанового сплаву за температури 0 °C в середовищі талого льоду. Характеристики механічних властивостей і вплив циклічного навантаження на функціональні властивості сплаву досліджували за одноосного розтягу циліндричних зразків діаметром 4 мм і довжиною робочої ділянки 12,5 мм, які були вирізані з прутка Ø8 мм. Частота навантаження за синусоїдальної форми циклу складала 0,5 Гц. Коефіцієнт асиметрії циклу навантаження  $r = s_{\min} / s_{\max} = 0$  (тут  $s_{\min}$ ,  $s_{\max}$  – найменше і найбільше значення переміщення штоку). При температурі вище температури закінчення мартенситно – аустенітного перетворення СПФ, в умовах контрольованого переміщення затискачів, вплив циклічного навантаження на максимальне напруження загалом можна охарактеризувати ділянками зміцнення, знеміцнення, стабілізації і стрімкого падіння максимального напруження, яке спричинене появою та поширенням макротріщини. Для усіх значень початкового максимального напруження, упродовж перших десяти циклів навантаження, спостерігається стрімке зменшення розмаху деформації, потім – ділянка стабілізації розмаху деформації або мени інтенсивного її зменшення, після якої йде ділянка спаду, що завершується руйнуванням зразка. Зі збільшенням максимального напруження у першому циклі навантаження від 509 МПа до 605 МПа збільшується значення розмаху деформації.

**Ключові слова:** NiTi сплав, псевдопружність, диференціальна сканувальна калориметрія, функціональні властивості, максимальні напруження, розмах деформації.

[https://doi.org/10.33108/visnyk\\_tntu2018.04.007](https://doi.org/10.33108/visnyk_tntu2018.04.007)

Отримано 09.01.2019